NASA TECHNICAL NOTE

NASA TN D-5501

INJECTION OF AN ATTACHED INVISCID JET AT AN OBLIQUE ANGLE TO A MOVING STREAM

by Marvin E. Goldstein and Willis Braun

Lewis Research Center
Cleveland, Ohio

NATIONAL AERONAUTICS AND SPACE ADMINISTRATION • WASHINGTON, D. C. • OCTOBER 1969

1. Report No. NASA TN D-5501	2. Government Accession No.	3. Recipient's Catalog No.
4. Title and Subtitle INJECTION OF AN ATTACHED INVISCID JET AT AN OBLIQUE ANGLE TO A MOVING STREAM		5. Report Date October 1969 6. Performing Organization Code
7. Author(s) Marvin E. Goldstein and Willis Braun		8. Performing Organization Report No. E-5106
9. Performing Organization Name and Address Lewis Research Center National Aeronautics and Space Administration Cleveland, Ohio 44135		10. Work Unit No. 129-01 11. Contract or Grant No.
12. Sponsoring Agency Name and Address National Aeronautics and Space Administration Washington, D.C. 20546		13. Type of Report and Period Covered Technical Note 14. Sponsoring Agency Code

15. Supplementary Notes

16. Abstract

An analytical solution has been obtained to the problem of a two-dimensional inviscid, incompressible jet injected into a moving stream from an orifice set at an oblique angle to the stream for the case where the jet does not separate from the downstream edge of the orifice. The solution is valid when the difference between the total pressure in the jet and the total pressure in the main stream is not too large. Typical flow patterns are presented to illustrate the effects of varying both the orifice angle and the total pressure within the jet.

17. Key Words *(Suggested by Author(s))* Jet injection Inviscid flow Conformal mapping	18. Distribution Statement Unclassified - unlimited		
19. Security Classif. (of this report) Unclassified	20. Security Classif. (of this page) Unclassified	21. No. of Pages 39	22. Price* $3.00

*For sale by the Clearinghouse for Federal Scientific and Technical Information
Springfield, Virginia 22151

INJECTION OF AN ATTACHED INVISCID JET AT AN OBLIQUE ANGLE TO A MOVING STREAM

by Marvin E. Goldstein and Willis Braun

Lewis Research Center

SUMMARY

An analytical solution has been obtained to the problem of a two-dimensional inviscid, incompressible jet injected into a moving stream from an orifice set at an oblique angle to the stream for the case where the jet does not separate from the downstream edge of the orifice. The solution is valid when the difference between the total pressure in the jet and the total pressure in the main stream is not too large. Typical flow patterns are presented to illustrate the effects of varying both the orifice angle and the total pressure within the jet.

INTRODUCTION

The flow field resulting from the oblique penetration of a jet into a flowing stream is of considerable interest in a number of fluid mechanical devices. Among these are ground-effects machines, jet flaps, wing fans, and fuel injection systems.

The dynamics of jet injection into moving streams is by no means fully understood. However, a certain amount of insight into this phenomenon can be gained by considering the injection of two-dimensional inviscid jets into flowing streams since flows of this type are simple enough to be amenable to mathematical analysis. It is realized that viscous effects can be significant in real flows. In order to take viscous effects into account, however, it is necessary to first perform an inviscid analysis and then modify the flow by superimposing viscous boundary layers. In any event, it is hoped that the inviscid analysis will reveal some of the significant features of the flow and thereby lead to an increased understanding of the phenomena involved. The work done along these lines to date is summarized in reference 1.

In reference 1 a technique was developed and applied to obtain an explicit analytic solution for the flow field resulting from a two-dimensional inviscid and incompressible

jet issuing from an orifice into a moving stream. The orifice was at an oblique angle to the stream and it was assumed that the jet separates from the downstream edge of the orifice to form a stagnant wake. Since it is not possible to tell from the inviscid analysis whether the jet will separate, remain attached, or form a separation bubble, it is also of interest to consider the flow that would result if no separation occurred. Hence, in this report the techniques used in reference 1 are used to obtain a solution for the case where the jet does not separate from the downstream edge of the orifice. The flow configuration is shown in figure 1 (p. 5). Since no separation is allowed to occur, it is necessary to allow the velocity to become infinite at the downstream edge of the orifice. This condition is approximately realized in certain real flows. The usual method for handling this situation is to replace the boundary streamline by one which is close to it when interpreting the results (ref. 2). In the present case this corresponds to replacing the infinitely thin plate which forms the downstream edge of the orifice by one of finite thickness with a streamlined leading edge.

As in reference 1, the flow will be assumed to be two-dimensional, inviscid, and incompressible. In addition, it will be required that in a certain sense (to be specified more precisely) the difference between the total pressure in the jet and the total pressure in the main stream be small. The upstream boundary of the jet is the streamline emanating from the upstream edge of the orifice.

The problem is solved by expanding the solutions in a small parameter related to the difference in total pressure between the jet and the mainstream. The zeroth-order solution corresponds to equal total pressures.

Since the boundary shapes for the first-order problem are unknown, a technique similar to that employed in thin airfoil theory is used to transform the first-order boundary conditions to the zeroth-order boundary. The solution is then obtained by using the theory of sectionally analytic functions.

It is proved in the appendix of reference 1 that the solution obtained herein also applies to the case where the density of the fluid in the jet differs from that in the mainstream.

SYMBOLS

A horizontal distance between edges of orifice

a A/l

B vertical distance between edges of orifice

b B/l

C_{ps} pressure coefficient along slip line

$D^{\pm}$ flow regions in physical plane

$\mathscr{D}_0^{\pm}$ regions in T-plane

H asymptotic jet width

h H/ℓ

I function defined by eq. (54)

J function defined by eq. (55)

ℓ characteristic length (set equal to H_0)

M function defined by eq. (63)

O order symbol

o order symbol

P total pressure in main stream

P_j total pressure in jet

P_∞ total pressure in main stream

P.V. Cauchy principal value

p static pressure

p_o static pressure at jet source (far inside the orifice)

p_∞ static pressure far upstream from jet

Q volume flow through jet

S slip line in physical plane

$\hat{S}$ distance along slip line

$\mathscr{S}_0$ slip line in T-plane

T intermediate variable, $T = \xi + i\eta$

U X-component of velocity

u U/V_∞

V Y-component of velocity

V_s^+ velocity along slip line inside of jet

V_∞ free stream velocity

v V/V_∞

W dimensionless complex potential, $\varphi + i\psi$

X coordinate in physical plane

x X/l

Y coordinate in physical plane

y Y/l

z dimensionless complex physical coordinate, $x + iy$

z^S dimensionless coordinate of points on slip line

Γ function defined by eq. (49)

γ dummy variable to replace η

ϵ $\dfrac{P_j - P_\infty}{\frac{1}{2}\rho V_\infty^2}$

Δ location of downstream edge of orifice in T-plane

δ defined in fig. 7

ζ dimensionless complex conjugate velocity, $u - iv$

η coordinate in T-plane

Θ function defined by eq. (31)

Λ defined by eq. (58)

ξ coordinate in T-plane

ρ density

τ dummy variable in T-plane

Φ velocity potential

φ Φ/lV_∞

Ψ stream function

ψ Ψ/lV_∞

Subscripts:

0 zeroth-order quantity

1 first-order quantity

Superscripts:

S value of quantity on slip line

+ value of quantity inside jet and orifice

- value of quantity in main stream

$\bar{}$ (overbar) complex conjugate

ANALYSIS

Formulation and Boundary Conditions

It will be assumed that the flow is inviscid, incompressible, and irrotational. The jet configuration is illustrated in figure 1. The analysis is limited to the case in which the difference between the total pressure in the jet P_j and the total pressure in the main stream P_∞ is not too large; or more specifically, to the case in which

$$|\epsilon| \ll 1$$

where

$$\epsilon \equiv \frac{P_j - P_\infty}{\frac{1}{2}\rho V_\infty^2} \tag{1}$$

ρ is the density of the fluid and V_∞ is the velocity of the main stream at infinity.

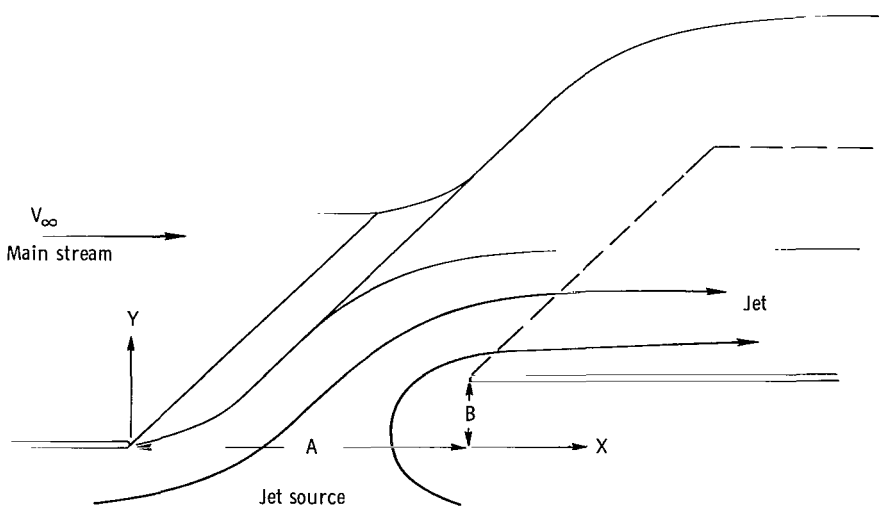

Figure 1. - Jet penetrating stream.

Let l be a convenient reference length which will be specified in the course of the analysis. The X and Y components of the velocity, U and V, respectively, will be made dimensionless by V_∞; and the stream function Ψ and the velocity potential Φ will be made dimensionless by $V_\infty l$. Thus, the dimensionless quantities u, v, ψ, and φ are defined by

$$u \equiv \frac{U}{V_\infty}$$

$$v \equiv \frac{V}{V_\infty}$$

$$\psi \equiv \frac{\Psi}{V_\infty l}$$

$$\varphi \equiv \frac{\Phi}{V_\infty l}$$

The dimensionless complex conjugate velocity ζ and the dimensionless complex potential W are defined, as usual, by

$$\zeta = u - iv$$

and

$$W = \varphi + i\psi$$

With all lengths made dimensionless by l (i.e., $x = X/l$, $y = Y/l$, $a = A/l$, $b = B/l$, and $h = H/l$) the flow configuration is shown in the physical plane (with the complex variable z defined by $z = x + iy$) in figure 2.

The stream of fluid issuing from the orifice formed by the two parallel walls $\overset{\frown}{HD}$ and $\overset{\frown}{EH}$ meets the main stream at the point D and forms a common streamline which is denoted by S in figure 2. The jet does not separate from the wall $\overset{\frown}{EH}$ at the point E but turns and flows back along $\overset{\frown}{EC}$. As a result of using this model it is necessary to allow the velocity to become infinite at the point E. Points on the common streamline will be denoted by $z^S = x^S + iy^S$.

In order to satisfy the requirement that there be no discontinuities in static pressure anywhere within the flow field, it is necessary (as is shown in ref. 1) to allow the velocity to be discontinuous across S. For this reason the streamline S will be called the

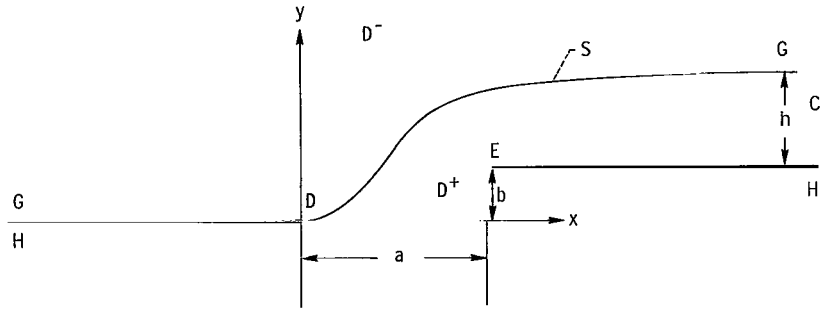

Figure 2. - Physical plane (z-plane).

slip line. The region within the jet and orifice is denoted by D^+ and the remaining region of the flow (i.e., the main stream) by D^-. Since the velocity (and as a consequence, the velocity potential) is discontinuous across S, it is convenient to use a superscript + to denote the flow quantities inside the jet (i.e., in D^+) and a superscript - to denote those in the main stream. Thus,

$$\zeta(z) = \begin{cases} \zeta^+(z) & \text{for } z \in D^+ \\ \zeta^-(z) & \text{for } z \in D^- \end{cases}$$

and

$$W(z) = \begin{cases} W^+(z) & \text{for } z \in D^+ \\ W^-(z) & \text{for } z \in D^- \end{cases}$$

Then ζ^+ and W^+ are holomorphic in the interior of D^+ and ζ^- and W^- are holomorphic in the interior of D^-.

A repetition of the argument given in reference 1 shows that Bernoulli's equation implies that

$$\left|\zeta^+(z^S)\right|^2 - \left|\zeta^-(z^S)\right|^2 = \frac{P_j - P_\infty}{\frac{1}{2}\rho V_\infty^2} = \epsilon \qquad (2)$$

at every point z^S of S. Since S is a common streamline to the internal and external flows, it is clear that $\mathcal{I}m\, W^+(z^S)$ and $\mathcal{I}m\, W^-(z^S)$ are both constants. Moreover, the ar-

bitrariness in the definition of W can be partially removed by choosing these constants to be zero (ref. 3). Hence,

$$\mathcal{I}m\, W^{+}(z) = \mathcal{I}m\, W^{-}(z) = 0 \qquad \text{for} \quad z \in S \tag{3}$$

The remaining arbitrariness in W can be removed by choosing

$$W^{+}(0) = W^{-}(0) = 0 \tag{4}$$

The conditions imposed on the velocity at infinity are (in view of the manner of nondimensionalization)

$$\zeta^{+}(z) \to 0 \qquad \text{for} \quad z \to H \tag{5}$$

$$\zeta^{-}(z) \to 1 \qquad \text{for} \quad z \to G \tag{6}$$

The remaining boundary conditions are that the normal component of the velocity vanish on the solid boundaries. These conditions are sufficient to completely determine the solution. They are summarized below for convenient reference.

$$\left.\begin{aligned} &\left|\zeta^{+}(z)\right|^{2} - \left|\zeta^{-}(z)\right|^{2} = \epsilon \\ &\mathcal{I}m\, W^{+}(z) = \mathcal{I}m\, W^{-}(z) = 0 \end{aligned}\right\} \text{for} \quad z \in S$$

$$\left.\begin{aligned} &\mathcal{I}m\, \zeta^{+}(z) = 0; \qquad z \in \overset{\frown}{EC} \\ &\mathcal{I}m\, \zeta^{+}(z) = 0; \qquad z \in \overset{\frown}{HD} \\ &\mathcal{I}m\, \zeta^{+}(z) = 0; \qquad z \in \overset{\frown}{EH} \\ &\mathcal{I}m\, \zeta^{-}(z) = 0; \qquad z \in \overset{\frown}{GD} \end{aligned}\right\} \tag{7}$$

Asymptotic Expansions

For small values of ϵ the functions $\zeta^{\pm}$ and $W^{\pm}$ can be expanded in an asymptotic power series in ϵ. In view of the fact that the shape of the slip line depends on ϵ, these expansions imply that the coordinates of S, z^{S}, and the asymptotic jet width h must also be expanded in powers of ϵ. Hence,

$$\left.\begin{aligned} \zeta^{\pm} &= \zeta_0 + \epsilon\zeta_1^{\pm} + \cdots \\ W^{\pm} &= W_0 + \epsilon W_1^{\pm} + \cdots \\ z^S &= z_0^S + \epsilon z_1^S + \cdots \\ h &= h_0 + \epsilon h_1 + \cdots \end{aligned}\right\} \tag{8}$$

As pointed out in reference 1 the expansion of z^S does not imply that the complex variable z is being expanded. It is also shown in reference 1 that the coefficients in the expansion of $\zeta^{\pm}$ are related to those in the expansion of $W^{\pm}$ by

$$\left.\begin{aligned} \zeta_0 &= \frac{dW_0}{dz} \\ \zeta_1^{\pm} &= \frac{dW_1^{\pm}}{dz} \\ &\cdots \\ &\cdots \\ &\cdots \end{aligned}\right\} \tag{9}$$

The reason for omitting the superscript + or - in the zeroth-order terms of the first two expansions is that (as will be shown subsequently) the zeroth-order solutions are not discontinuous across the curve S and so there is a single function ζ_0 which is holomorphic in the entire flow field (of course, the same is true for W_0).

The reference length ℓ will now be chosen in such a way that

$$h_0 = 1$$

Thus ℓ is the zeroth-order asymptotic thickness of the jet. This is denoted symbolically by putting

$$\ell = H_0 \tag{10}$$

The last expansion (eq. (8)) is then

$$h = 1 + \epsilon h_1 + \ldots \tag{11}$$

Zeroth-Order Solution

When the expansions (eq. (8)) are substituted into the boundary conditions (eqs. (4) to (7)) and only the zeroth-order terms are retained, the following boundary conditions for the zeroth-order solution are obtained: First, the first boundary condition (eq. (7)) shows, as has already been anticipated, that the zeroth-order solution must be continuous across the slip line, and, hence, that it is characterized by functions which are holomorphic everywhere within the flow field. The remaining conditions show that

$$\left.\begin{aligned} W_0(0) &= 0 \\ \mathcal{I}m\, W_0\left(z_0^S\right) &= 0 \end{aligned}\right\} \tag{12}$$

$$\left.\begin{aligned} \mathcal{I}m\, \zeta_0(z) = 0 \quad \text{for} \quad & \begin{cases} z \in EC \\ z \in HD \\ z \in EH \\ z \in GD \end{cases} \\ \zeta_0(z) \to 0 \quad & \text{for} \quad z \to H \\ \zeta_0(z) \to 1 \quad & \text{for} \quad z \to G \end{aligned}\right\} \tag{13}$$

The conditions (eq. (12)) merely serve to show that because of the manner in which the arbitrary constants have been adjusted in the complex potential the streamline emanating from the point D is to be taken as the zero streamline.

Now the change in the stream function across the jet must be equal to the volume flow rate through the jet. Hence, if Q_0 denotes the dimensionless zeroth-order volume flow through the jet, and $\Delta\psi_0$ denotes the zeroth-order change in the stream function across the jet, it is clear from the definition of stream function that

$$Q_0 = \Delta\psi_0$$

The last boundary condition (eq. (13)) shows that far downstream in the jet (i.e., at the point C) the zeroth-order velocity goes to 1. In view of the normalization (eq. (11)) the asymptotic thickness of this portion of the jet must also be 1. It follows from these remarks that $Q_0 = 1$. Hence,

$$\Delta\psi_0 = 1 \tag{14}$$

Now the boundary value problem posed by the boundary conditions (eq. (13)) is a simple free streamline problem which can be readily solved by the Helmholtz-Kirchoff technique. In fact, the solution to this problem has already been carried out by Ehrich (ref. 4). His solution, however, is somewhat inconvenient for our purposes. Thus, it will be necessary to use a slightly different approach in order to obtain a zeroth-order solution which is in a convenient form to use for calculating the higher-order terms. The procedure for obtaining the solution is (ref. 3), of course, to draw the region of flow in the hodograph plane and in the complex potential plane, and then to find the appropriate mapping of these two planes into some convenient intermediate plane (say, the T-plane). The shapes of these regions can readily be deduced from the boundary conditions (eq. (13)), and they are shown in figures 3 and 4 (we have put $W_0 = \varphi_0 + i\psi_0$ in fig. 3). The corresponding points in the various planes are designated by the same letters. The zeroth-order "slip line" is shown dashed in these figures since it does not correspond to a line of discontinuity and can therefore be ignored as far as obtaining the zeroth-order solution is concerned. The intermediate T-plane is chosen in such a way

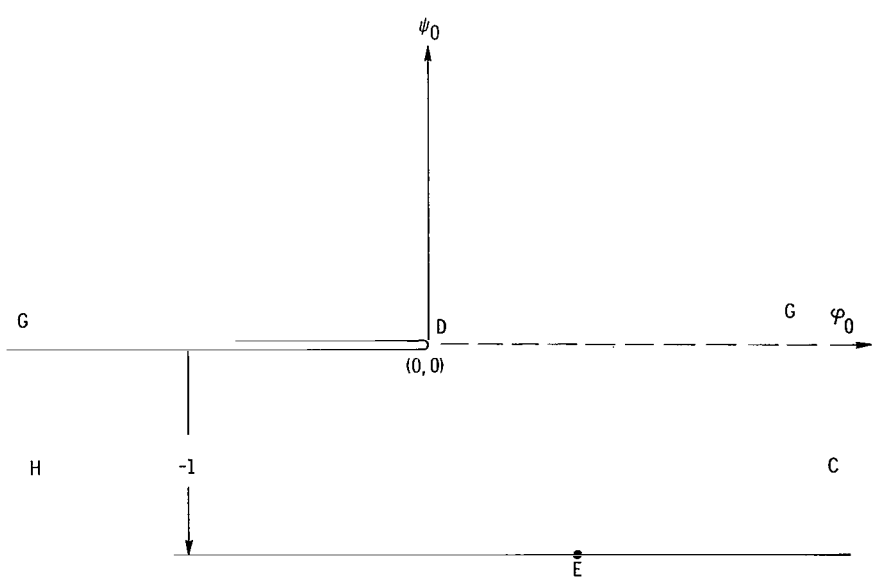

Figure 3. - Zeroth-order complex potential plane (W_0-plane).

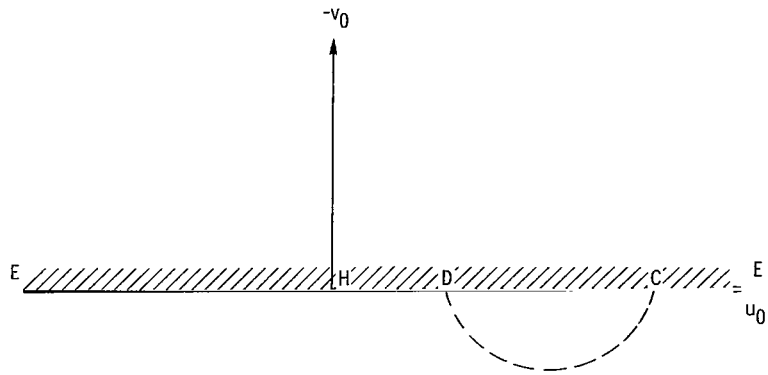

Figure 4. - Zeroth-order hodograph (ζ_0-plane).

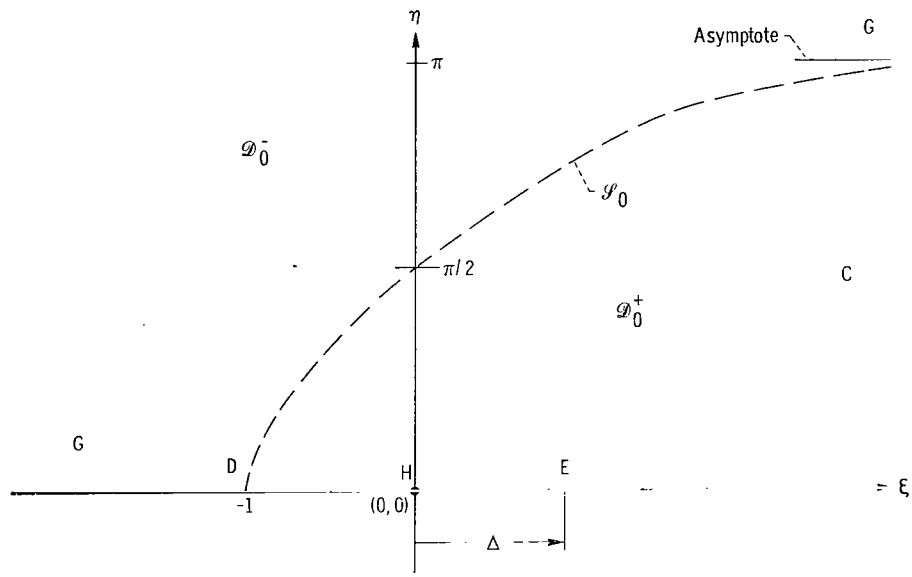

Figure 5. - Intermediate plane (T-plane).

that the region of flow maps into the upper half plane in the manner indicated in figure 5. We shall denote the real and imaginary parts of the variable T by ξ and η, respectively. The region of the T-plane into which the zeroth-order flow field interior to the jet maps is denoted by $\mathscr{D}_0^+$, and the region of the T-plane into which the zeroth-order main stream maps is denoted by $\mathscr{D}_0^-$. The dividing line between these two regions (which is being called for convenience the zeroth-order slip line even though no slip occurs in the zeroth-order solution) is denoted by $\mathscr{S}_0$.

Simple applications of the Schwartz-Christoffel and linear fractional transformation (ref. 5) show that the mappings which properly transform the W_0-plane and the ζ_0-plane into the upper half T-plane in the manner indicated in the figures are respectively

defined by

$$\frac{dW_0}{dT} = \frac{1}{\pi}\,\frac{T+1}{T} \qquad \text{for } \eta \geq 0 \tag{15}$$

and

$$\zeta_0 = \frac{T}{T-\Delta} \qquad \text{for } \eta \geq 0 \tag{16}$$

or, performing the indicated integration,

$$W_0 = \frac{1}{\pi}(T + 1 + \ln T) - i \qquad \text{for } \eta \geq 0$$

Since the W_0-plane and the T-plane are essentially the same as those of reference 1, the results obtained therein can be used to show that the parametric equation for the zeroth-order slip line $\mathscr{S}_0$ in the T-plane is

$$T = -\frac{\eta}{\tan \eta} + i\eta = -\frac{\eta}{\sin \eta}\,e^{-i\eta} \qquad \text{for } 0 < \eta < \pi \tag{17}$$

It follows from the first equation (9) that the points in the physical plane (fig. 2) are related to the points in the T-plane by

$$z(T) = \int \frac{1}{\zeta_0(T)}\,\frac{dW_0}{dT}\,dT + \text{Constant} \tag{18}$$

Substituting equations (15) and (16) into this formula and using the fact, indicated in figure 2, that the origin of the coordinate system in the physical plane is to be at the point D result in

$$z(T) = \frac{1}{\pi}\int_{-1}^{T} \frac{(T-\Delta)(T+1)}{T^2}\,dT$$

$$= \frac{1}{\pi}\left[T + (1-\Delta)\ln T + \frac{\Delta}{T} + (1+\Delta)\right] + (\Delta - 1)i \tag{19}$$

By definition (see figs. 2 and 5)

$$z(\Delta) = a + ib$$

Hence, equation (19) shows

$$a + ib = \frac{1}{\pi}\left[(1 - \Delta)\ln \Delta + 2(1 + \Delta)\right] + i(\Delta - 1)$$

Therefore, on equating real and imaginary parts,

$$\left.\begin{aligned} a &= \frac{1}{\pi}\left[(1 - \Delta)\ln \Delta + 2(1 + \Delta)\right] \\ b &= \Delta - 1 \end{aligned}\right\} \tag{20}$$

Formulation of First-Order Problem in Physical Plane

The mapping $T \rightarrow Z$ defined by equation (19) maps the upper half T-plane approximately into the region of flow in the physical plane. The domain $\mathscr{D}_0^+$ is mapped into the crosshatched region of the physical plane shown in figure 6. The curve $\mathscr{S}_0$ is mapped into the dashed boundary S_0 of this region. This region, of course, differs from the true interior of the jet whose boundary S is indicated by the solid line (curved) in figure 6.

Now the first group of the boundary conditions (eq. (7)) is specified on the curve S in the physical plane, whose shape is not known at this stage of the solution. As explained in reference 1, however, these boundary conditions, correct to terms of the order ϵ, can be transferred to S_0 by relating the values of $\zeta^{\pm}$ and $W^{\pm}$ at an arbitrary point z^S of S to their values at some neighboring point z_0^S of S_0 by performing

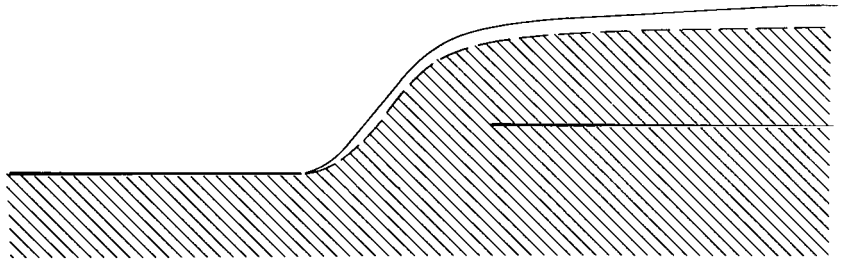

Figure 6. - Comparison as zeroth order and true jet boundaries in physical plane.

a Taylor series expansion of these quantities about z_0^S. Thus,

$$\zeta^{\pm}(z^S) = \zeta^{\pm}\left(z_0^S\right) + \left(\frac{d\zeta^{\pm}}{dz}\right)_{z=z_0^S}\left(z^S - z_0^S\right) + \cdots$$

$$W^{\pm}(z^S) = W^{\pm}\left(z_0^S\right) + \zeta^{\pm}\left(z_0^S\right)\left(z^S - z_0^S\right) + \cdots$$

As in reference 1 substitution of the asymptotic expansion (eq. (8)) into these Taylor series yields, after neglecting terms of $O(\epsilon^2)$,

$$\zeta^{\pm}(z^S) = \zeta_0\left(z_0^S\right) + \epsilon\left[\zeta_1^{\pm}\left(z_0^S\right) + \left(\frac{d\zeta_0}{dz}\right)_{z=z_0^S} z_1^S\right] + O(\epsilon^2) \tag{21}$$

$$W^{\pm}(z^S) = W_0\left(z_0^S\right) + \epsilon\left[W_1^{\pm}\left(z_0^S\right) + \zeta_0\left(z_0^S\right)z_1^S\right] + O(\epsilon^2) \tag{22}$$

And these expressions relate the values of the dependent variables $W^{\pm}$ and $\zeta^{\pm}$ at the points of the unknown boundary S to their values on the known boundary S_0 with an error of order ϵ^2. An easy calculation carried out in reference 1 shows that equation (21) implies

$$\left|\zeta^{\pm}(z^S)\right|^2 = \left|\zeta_0\left(z_0^S\right)\right|^2 + 2\epsilon\left|\zeta_0\left(z_0^S\right)\right|^2 Re\left[\frac{\zeta_1^{\pm}\left(z_0^S\right)}{\zeta_0\left(z_0^S\right)} + \frac{1}{\zeta_0\left(z_0^S\right)}\left(\frac{d\zeta_0}{dz}\right)_{z=z_0^S} z_1^S\right] + O(\epsilon^2) \tag{23}$$

Finally, substituting the expansions (eqs. (22) and (23)) into the first group of boundary conditions (eq. (7)) and equating the coefficients of ϵ to the first power yields the following first-order boundary conditions on the slip line:

$$Re\left[\frac{\zeta_1^+\left(z_0^S\right)}{\zeta_0\left(z_0^S\right)} - \frac{\zeta_1^-\left(z_0^S\right)}{\zeta_0\left(z_0^S\right)}\right] = \frac{1}{2}\,\frac{1}{\left|\zeta_0\left(z_0^S\right)\right|^2} \tag{24}$$

$$Im\left[W_1^+\left(z_0^S\right) + \zeta_0\left(z_0^S\right)z_1^S\right] = 0 \tag{25}$$

$$Im\left[W_1^-\left(z_0^S\right) + \zeta_0\left(z_0^S\right)z_1^S\right] = 0 \tag{26}$$

Thus, equations (24) to (26) are the boundary conditions for the first-order solutions on the boundary S "transferred" to the zeroth-order boundary S_0. Hence, the first-order boundary value problem has been transformed from one in which the shape of the boundaries is unknown to one in which it is known. Notice, however, that these boundary conditions involve the variables $W_1^{\pm}$, $\zeta_1^{\pm}$, and z_1^S. But, $\zeta_1^{\pm}$ is completely determined in terms of $W_1^{\pm}$ by the second equation (9). In view of this the conditions (eqs. (24) to (26)) may be thought of as two boundary conditions connecting the variable ζ_1^+ with the variable ζ_1^- across S_0 (or equivalently the variable W_1^+ with the variable W_1^-) plus an equation which determines z_1^S once $\zeta_1^{\pm}$ are known. Thus, subtracting equation (26) from (25) yields

$$\mathcal{I}m\, W_1^+\left(z_0^S\right) = \mathcal{I}m\, W_1^-\left(z_0^S\right) \tag{27}$$

Then in view of the second equation (9), equations (24) and (27) are the boundary conditions on S_0 which connect the solution ζ_1^+ in D^+ with the solution ζ_1^- in D^-, and equation (25) serves to determine z_1^S once ζ_1^+ is known (actually z_1^S will be determined in a slightly different fashion). It is shown in reference 1 that the boundary condition (eq. (27)) can be differentiated to obtain

$$\mathcal{I}m\left[\frac{\zeta_1^+\left(z_0^S\right)}{\zeta_0\left(z_0^S\right)} - \frac{\zeta_1^-\left(z_0^S\right)}{\zeta_0\left(z_0^S\right)}\right] = 0$$

Multiplying this by i and adding it to equation (24) yield the following single (complex) jump condition on S^o:

$$\frac{\zeta_1^+\left(z_0^S\right)}{\zeta_0\left(z_0^S\right)} - \frac{\zeta_1^-\left(z_0^S\right)}{\zeta_0\left(z_0^S\right)} = \frac{1}{2}\,\frac{1}{\left|\zeta_0\left(z_0^S\right)\right|^2} \tag{28}$$

The boundary conditions for the remaining (solid) boundaries are easily deduced by substituting the first asymptotic expansion (eq. (8)) into expressions (5) and (6) and the second group of boundary conditions (eq. (7)) and equating the coefficients of ϵ to the first power. Thus,

$$\left.\begin{aligned}
&\mathcal{I}m\ \zeta_1^+(z) = 0 \begin{cases} z \in \widehat{EC} \\ z \in \widehat{HD} \\ z \in \widehat{EH} \end{cases} \\
&\mathcal{I}m\ \zeta_1^-(z) = 0 \qquad z \in \widehat{GD} \\
&\zeta_1^+(z) \to 0 \qquad z \to H \\
&\zeta_1^-(z) \to 0 \qquad z \to G
\end{aligned}\right\} \tag{29}$$

Solution of First-Order Boundary-Value Problem

The boundary conditions (eqs. (28) and (29)) completely determine a boundary-value problem (or more precisely, two boundary-value problems connected along the curve S_0) for a holomorphic function in the region of flow in the physical plane. However, under the change of variable $z \to T$ defined by equation (19) this boundary-value problem can be transformed into one in the upper half T-plane (fig. 5). The boundary conditions in the T-plane are

$$\left.\begin{aligned}
&\frac{\zeta_1^+(T)}{\zeta_0(T)} - \frac{\zeta_1^-(T)}{\zeta_0(T)} = \frac{1}{2}\,\frac{1}{|\zeta_0(T)|^2} \qquad \text{for } T \in \mathcal{S}_0 \\
&\mathcal{I}m\ \zeta_1^+(\xi + i0) = 0 \qquad \text{for } \xi \geq -1 \\
&\mathcal{I}m\ \zeta_1^-(\xi + i0) = 0 \qquad \text{for } \xi \leq -1 \\
&\zeta_1^-(T) \to 0 \qquad \text{for } T \to \infty \\
&\zeta_1^+(0) = 0
\end{aligned}\right\} \tag{30}$$

Clearly, the domains of definition of ζ^+ and ζ^- are $\mathcal{D}_0^+$ and $\mathcal{D}_0^-$, respectively. It is convenient to work with the sectionally analytic function Θ defined on the upper half T-plane in terms of $\zeta^\pm$ by

$$\Theta(T) = \begin{cases} \Theta^+(T) \equiv \dfrac{\zeta_1^+(T)}{\zeta_0(T)} - \dfrac{1}{2} & \text{for } T \in \mathscr{D}_0^+ \\ \Theta^-(T) \equiv \dfrac{\zeta_1^-(T)}{\zeta_0(T)} + \dfrac{1}{2\zeta_0^2(T)} - \dfrac{1}{2} & \text{for } T \in \mathscr{D}_0^- \end{cases} \tag{31}$$

It follows from the boundary conditions (eq. (30)) that Θ must satisfy

$$\left.\begin{array}{ll} \Theta^+(T) - \Theta^-(T) = \Gamma(T) & \text{for } T \in \mathscr{S}^0 \\ \mathscr{I}m\, \Theta(\xi + i0) = 0 & \text{for } -\infty < \xi < +\infty \\ \Theta(T) \to 0 & \text{for } T \to \infty \end{array}\right\} \tag{32}$$

where we have put

$$\begin{aligned} \Gamma(T) &\equiv \frac{1}{2}\left[\frac{1}{|\zeta_0(T)|^2} - \frac{1}{\zeta_0^2(T)}\right] \\ &= \frac{1}{2\zeta_0(T)}\left[\frac{1}{\overline{\zeta_0(T)}} - \frac{1}{\zeta_0(T)}\right] \\ &= -\frac{i}{\zeta_0(T)}\,\mathscr{I}m\,\frac{1}{\zeta_0(T)} \end{aligned} \tag{33}$$

Since $\zeta_1^{\pm}$ can be no more singular than ζ_0, if the asymptotic expansion is to be uniformly valid it follows that Θ must be bounded on the real axis.

The function Θ can now be constructed as follows: An investigation of the behavior of $\Gamma(T)$ at $T = \infty$ and $T = -1$ shows that it vanishes at these points like some power of T. Hence, the Plemelj formulas (ref. 6) show that the Cauchy integral

$$\frac{1}{2\pi i}\int_{\mathscr{S}_0} \frac{\Gamma(\tau)}{\tau - T}\, d\tau \tag{34}$$

where the integration is to be performed along $\mathscr{S}_0$ in a counterclockwise direction

about $\mathscr{D}_0^+$) is a sectionally analytic function which is bounded on the real axis, vanishes at infinity, and satisfies the jump condition (eq. (30)). However, this function is not necessarily real for real values of T. But this can be compensated (as shown in ref. 6) by adding the function

$$-\frac{1}{2\pi i}\int_{\mathscr{S}_0}\frac{\overline{\Gamma(\tau)}\,\overline{d\tau}}{\overline{\tau}-T}$$

to equation (34). (Notice that, if f is holomorphic in the upper half plane, the function $\overline{f}$ defined by $\overline{f}(T) = \overline{f(\overline{T})}$ is also holomorphic there and $f(\xi) + \overline{f}(\xi) = f(\xi) + \overline{f(\xi)}$ is real.) Thus, the function Θ with the required properties is defined by

$$\Theta(T) \equiv \frac{1}{2\pi i}\int_{\mathscr{S}_0}\frac{\Gamma(\tau)d\tau}{\tau-T} - \frac{1}{2\pi i}\int_{\mathscr{S}_0}\frac{\overline{\Gamma(\tau)}\,\overline{d\tau}}{\overline{\tau}-T} \qquad \text{for } \mathcal{R}e\,T \geq 0 \tag{35}$$

In view of the mapping $T \to z$ defined by equation (19), this completes the solution of the problem since equation (31) determines $\zeta_1^{\pm}$ in terms of the known function Θ. It is also convenient to have an expression for $W_1^{\pm}$ in terms of Θ. To this end, notice that it follows from the first and second of equations (9) that

$$\zeta_1^{\pm} = \frac{dW_1^{\pm}}{dz} = \frac{dW_1^{\pm}}{dT}\frac{dT}{dW_0}\zeta_0$$

Hence,

$$\frac{dW_1^{\pm}}{dT} = \frac{dW_0}{dT}\frac{\zeta_1^{\pm}}{\zeta_0}$$

Using this in equation (31) shows that

$$\frac{dW_1^{+}}{dT} = \frac{dW_0}{dT}\Theta^{+}(T) + \frac{1}{2}\frac{dW_0}{dT} \tag{36}$$

$$\frac{dW_1^-}{dT} = \frac{dW_0}{dT}\,\Theta^-(T) + \frac{1}{2}\,\frac{dW_0}{dT}\left[1 - \frac{1}{\zeta_0^2(T)}\right] \tag{37}$$

Notice that $z = 0$ when $T = -1$ and, therefore, equation (4) implies that $W_1^{\pm}(T)$ both vanish at $T = -1$. Hence, integrating equations (36) and (37) between -1 and T yields

$$W_1^+(T) = \int_{-1}^{T} \Theta^+(T)\,\frac{dW_0}{dT}\,dT + \frac{1}{2}\,W_0(T) \tag{38}$$

$$W_1^-(T) = \int_{-1}^{T} \Theta^-(T)\,\frac{dW_0}{dT}\,dT + \frac{1}{2}\left[W_0(T) - \int_{-1}^{T} \frac{1}{\zeta_0^2(T)}\,\frac{dW_0}{dT}\,dT\right] \tag{39}$$

Let Q denote the dimensionless volume flow through the jet. It follows from the definition of the stream function that to within an error of $O(\epsilon^2)$

$$Q = \mathcal{I}m\left[W_0(-1 + i0) + \epsilon W_1^+(-1 + i0)\right] - \mathcal{I}m\left[W_0(\Delta + i0) + \epsilon W_1^+(\Delta + i0)\right] + O(\epsilon^2)$$

Or using equation (14) and the fact that $W_1^+(T)$ and $W_0(T)$ both vanish at $T = -1$ this becomes

$$Q = 1 - \epsilon\,\mathcal{I}m\,W_1^+(\Delta + i0) + O(\epsilon^2)$$

Substituting equation (38) into this expression and using equation (14) again shows that

$$Q = 1 + \frac{\epsilon}{2} - \epsilon\,\mathcal{I}m \int_{-1}^{\Delta} \Theta^+(T)\,\frac{dW_0}{dT}\,dT + O(\epsilon^2)$$

Or substituting in equation (15) this becomes

$$Q = 1 + \frac{\epsilon}{2} - \frac{\epsilon}{\pi}\,\mathcal{I}m \int_{-1}^{\Delta} \Theta^+(T)\,\frac{T+1}{T}\,dT + O(\epsilon^2) \tag{40}$$

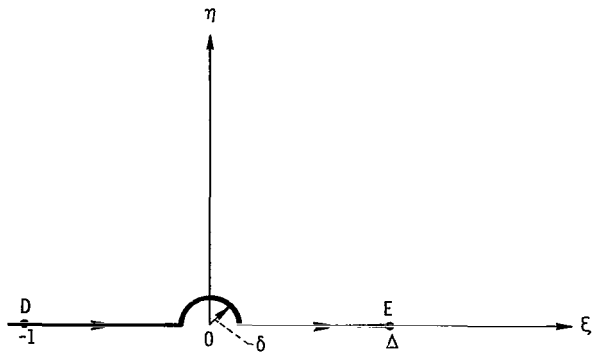

Figure 7. - Path of integration for $\frac{1}{\pi}\int_{-1}^{\Delta}\Theta^{+}(T)\,\frac{T+1}{T}\,dT$ in T-plane.

In view of the singularity in the denominator this integral must first be carried out over the path shown in figure 7 and then the limit $\delta \to 0$ can be taken. Performing these operations yields

$$\frac{1}{\pi}\int_{-1}^{\Delta}\Theta^{+}(T)\,\frac{T+1}{T}\,dT = \frac{P.V.}{\pi}\int_{-1}^{\Delta}\Theta^{+}(\xi)\,\frac{\xi+1}{\xi}\,d\xi - i\Theta^{+}(0)$$

where P.V. denotes the Cauchy principal value. Because $\Theta^{+}(\xi + i0)$ is real, equation (40) becomes

$$Q = 1 + \frac{\epsilon}{2} = \epsilon\Theta^{+}(0) + O(\epsilon^{2}) \tag{41}$$

Since the flow far downstream in the jet becomes uniform and since $\lim_{z\to\infty}\zeta^{-}(z) = 1$, it follows from equation (2) (see fig. 2)

$$\lim_{z\to c}\zeta^{+}(z) = \sqrt{1+\epsilon}$$

Therefore, continuity requirements dictate that the dimensionless net volume flow through the jet Q be equal to

$$h\sqrt{1+\epsilon}$$

Expanding this in powers of ϵ we find with the aid of the expansion (eq. (11))

$$Q = (1 + \epsilon h_1 + \ldots)\left(1 + \frac{1}{2}\epsilon + \ldots\right)$$

$$= 1 + \epsilon\left(\frac{1}{2} + h_1\right) + \ldots \tag{42}$$

Hence, equating like powers of ϵ in equations (41) and (42) shows that

$$h_1 = \Theta^+(0) \tag{43}$$

Since equation (19) set up a one-to-one correspondence between points of the physical plane and points of the T-plane, it is clear that equations (31), (35), (38), and (39) can be used to compute the first-order perturbation to the velocity and stream function at each point of the physical plane.

In view of the fact that once the shape of the jet is known it is quite easy to sketch in the streamline patterns, the most important quantities to be obtained from the analysis are the shapes of the curve S in the physical plane (see fig. 2). However, since the viscous spreading of the jet is controlled by the pressure (or equivalently, the velocity) distribution along the slip line S, that quantity is also of some importance. Hence, explicit formulas will now be obtained for these quantities by using the formulas previously derived.

Computation of Boundary Values

In view of the one-to-one nature of the mapping involved it is clear that, if $\mathcal{I}m\, W^+(z) = 0$, then z must be a point on the streamline which passes through the point D in figure 2. In addition, since the velocity potential is increasing in the direction D → C along S, it is clear that, if $\mathcal{R}e\, W^+(z) > \mathcal{R}e\, W^+(0) = 0$ (see eq. (4)), then z must be a point of the slip line S. It is clear that $\mathcal{I}m\, W_0(z_0^S) = 0$ and $\mathcal{R}e\, W_0(z_0^S) \geq 0$ for any point $z_0^S \in S_0$. In view of these considerations it follows that the point $z^S = z_0^S + \epsilon z_1^S$ will be on the first-order position of S if z^S satisfies the equation

$$W^+(z^S) = W_0\left(z_0^S\right)\left(1 + \frac{\epsilon}{2}\right) \tag{44}$$

It is clear from this equation that when $z_0^S = 0$, $W^+(z^S) = 0$, and that $\mathcal{R}e\, W^+(z^S) \to \infty$ as $z_0^S \to \infty$. Hence, the point z^S traverses the streamline S as z_0^S traverses the zeroth-order slip line S_0.

By substituting equation (44) into the expansion (eq. (22)), the first-order distance z_1^S from the zeroth-order slip line to the slip line is found to be

$$z_1^S = -\frac{1}{\zeta_0(T)}\left[W_1^+(T) - \frac{1}{2}W_0(T)\right] \qquad \text{for } T \in \mathscr{S}_0 \tag{45}$$

where the fact has been used that the curve S_0 in the physical plane is the conformal image under the mapping $T \to z$ defined in equation (19) of the curve $\mathscr{S}_0$ in the T-plane. This also shows that

$$z^S = z(T) + \epsilon z_1^S + O(\epsilon^2) \qquad \text{for } T \in \mathscr{S}_0 \tag{46}$$

In addition, equation (23) shows that the magnitude of the velocity at each point z^S of the slip line is given to within terms of order ϵ^2 by

$$\left|\zeta^+(z^S)\right|^2 = \left|\zeta_0(T)\right|^2 + 2\epsilon\left|\zeta_0(T)\right|^2 \mathcal{R}e\left[\frac{\zeta_1^+(T)}{\zeta_0(T)} + \frac{1}{\zeta_0(T)}\frac{d\zeta_0}{dz}z_1^S\right] \qquad \text{for } T \in \mathscr{S}_0 \tag{47}$$

Substituting equation (45) into (46) and substituting equation (38) into the resulting expression yield

$$z^S = z(T) - \frac{\epsilon}{\zeta_0(T)}\int_{-1}^{T}\Theta^+(T)\frac{dW_0}{dT}\,dT \qquad \text{for } T \in \mathscr{S}_0 \tag{48}$$

where the integral can be taken along the curve $\mathscr{S}_0$ if $\Theta^+(T)$ is interpreted as the limiting value of $\Theta(T)$ as T approaches $\mathscr{S}_0$ from within $\mathscr{D}_0^+$.

It follows from the first equation (9) and equations (46), (48), and (31) that

$$\frac{\zeta_1^+(T)}{\zeta_0(T)} + \frac{1}{\zeta_0(T)}\frac{d\zeta_0}{dz}z_1^S = \frac{\zeta_1^+(T)}{\zeta_0(T)} + \frac{d\zeta_0}{dW_0}z_1^S$$

$$= \frac{1}{2} + \Theta^+(T) - \frac{d\ln\zeta_0}{dW_0}\int_{-1}^{T}\Theta^+(T)\frac{dW_0}{dT}\,dT$$

Substituting this into equation (47) shows that

$$|\zeta^+(z^S)|^2 = |\zeta_0(T)|^2 \left\{ 1 + \epsilon \right.$$

$$\left. + 2\epsilon \, \mathcal{R}e \left[\Theta^+(T) - \frac{d \ln \zeta_0}{dW_0} \int_{-1}^{T} \Theta^+(T) \frac{dW_0}{dT} \, dT \right] \right\} \qquad \text{for } T \in \mathcal{S}_0 \qquad (49)$$

The distance $\hat{S}$ measured along the curve S is given by

$$\hat{S} = H_0 \int_{-1}^{T} \left| \frac{dz^S}{dT} \right| |dT| \qquad \text{for } T \in \mathcal{S}_0 \qquad (50)$$

where the integral is taken along the curve $\mathcal{S}_0$. Now differentiating equation (46) and inserting equation (45) yield

$$\frac{dz^S}{dT} = \frac{dz}{dT} + \frac{\epsilon}{\zeta_0^2} \frac{d\zeta_0}{dT} \left(W_1^+ - \frac{1}{2} W_0 \right) - \frac{\epsilon}{\zeta_0} \left(\frac{dW_1^+}{dW_0} - \frac{1}{2} \right) \frac{dW_0}{dT}$$

$$= \frac{1}{\zeta_0} \frac{dW_0}{dT} \left[1 + \frac{\epsilon}{2} - \epsilon \left(\frac{\zeta_1^+}{\zeta_0} + \frac{d\zeta_0}{dz} \frac{1}{\zeta_0} z_1^S \right) \right]$$

Comparing this with equation (47) shows that

$$\left| \frac{dz^S}{dT} \right| = \left(1 + \frac{\epsilon}{2} \right) \left| \frac{dW_0}{dT} \right| \frac{1}{|\zeta^+(z^S)|}$$

Substituting this result into equation (50) shows that

$$\frac{\hat{S}}{H_0} = \left(1 + \frac{\epsilon}{2} \right) \int_{-1}^{T} \left| \frac{dW_0}{dT} \right| \frac{1}{|\zeta^+(z^S)|} |dT| \qquad (51)$$

All necessary results have now been obtained. However, it is convenient to rewrite some of these in more explicit form.

Explicit Formulas for Calculating Boundary Values

Substituting equation (16) into equation (33) yields

$$\Gamma(T) = -i\,\frac{T - \Delta}{T}\,\mathcal{I}m\,\frac{T - \Delta}{T}$$

Or using equation (17)

$$\Gamma(\eta) = -i(\eta + \Delta \sin \eta\, e^{i\eta})\Delta\left(\frac{\sin \eta}{\eta}\right)^2 \qquad \text{for } 0 \leq \eta < \pi \tag{52}$$

where $\Gamma(\eta)$ is used in place of $\Gamma\left[-(\eta/\sin \eta)e^{-i\eta}\right]$. Applying the Plemelj formulas (ref. 6) to equation (35) shows that

$$\Theta^+(T) = \frac{1}{2}\,\Gamma(T) + \frac{P.V.}{2\pi i}\int_{\mathcal{S}_0} \frac{\Gamma(\tau)d\tau}{\tau - T} - \frac{1}{2\pi i}\int_{\mathcal{S}_0} \frac{\overline{\Gamma(\tau)}\,\overline{d\tau}}{\overline{\tau} - T} \qquad \text{for } T \in \mathcal{S}_0$$

where the integration is to be performed in a counterclockwise direction along $\mathcal{S}_0$. In view of equation (24), however, this can be written as

$$\Theta^+(\eta) = \frac{1}{2}\,\Gamma(\eta) + \frac{P.V.}{2\pi i}\int_{\pi}^{0} \frac{\Gamma(\gamma)}{\frac{\gamma}{\sin \gamma}e^{-i\gamma} - \frac{\eta}{\sin \eta}e^{-i\eta}}\,d\left(\frac{\gamma}{\sin \gamma}e^{-i\gamma}\right)$$

$$- \frac{1}{2\pi i}\int_{\pi}^{0} \frac{\overline{\Gamma(\gamma)}}{\frac{\gamma}{\sin \gamma}e^{i\gamma} - \frac{\eta}{\sin \eta}e^{-i\eta}}\,d\left(\frac{\gamma}{\sin \gamma}e^{i\gamma}\right) \qquad \text{for } 0 \leq \eta < \pi$$

where, for brevity, $\Theta^+(\eta)$ is used in place of $\Theta^+\left[(-\eta/\sin \eta)e^{-i\eta}\right]$. Since

$$d\left(\frac{\gamma}{\sin\gamma}\, e^{-i\gamma}\right) = -\left(\frac{\gamma - \cos\gamma \sin\gamma}{\sin^2\gamma} + i\right)d\gamma \tag{53}$$

the foregoing equation can be written as

$$\Theta^+(\eta) = \frac{1}{2}\,\Gamma(\eta) + \frac{P.V.}{2\pi i}\int_0^{\pi} \frac{\Gamma(\gamma)\left[\frac{1}{\sin^2\gamma}(\gamma - \cos\gamma \sin\gamma) + i\right]d\gamma}{\gamma \cot\gamma - \eta \cot\eta - i(\gamma - \eta)}$$

$$- \frac{1}{2\pi i}\int_0^{\pi} \frac{\overline{\Gamma(\gamma)}\left[\frac{1}{\sin^2\gamma}(\gamma - \cos\gamma \sin\gamma) - i\right]d\gamma}{\gamma \cot\gamma - \eta \cot\eta + i(\gamma + \eta)} \qquad \text{for } 0 \le \eta < \pi \tag{54}$$

For $T = 0$ equation (35) becomes

$$\Theta^+(0) = -\frac{1}{\pi}\,\mathcal{I}m \int_0^{\pi} \Gamma(\gamma)\left(\frac{1}{\gamma} - \cot\gamma - i\right)d\gamma \tag{55}$$

Upon defining $z_0^S(\eta)$ and $\zeta_0^S(\eta)$ by

$$\left.\begin{aligned} z_0^S(\eta) &\equiv z\left(\frac{-\eta}{\sin\eta}\, e^{-i\eta}\right) \\ \zeta_0^S(\eta) &= \zeta_0\left(\frac{-\eta}{\sin\eta}\, e^{-i\eta}\right) \end{aligned}\right\} \qquad \text{for } 0 \le \eta < \pi \tag{56}$$

and using equations (15), (17), and (53), equation (46) becomes

$$z^S = z_0^S(\eta) - \epsilon\,\frac{I(\eta)}{\zeta_0^S(\eta)} \qquad \text{for } 0 \le \eta < \pi \tag{57}$$

where

$$I(\eta) \equiv \int_0^{\eta} \Theta^+(\gamma) J(\gamma) d\gamma \qquad \text{for } 0 \leq \eta < \pi \tag{58}$$

and

$$J(\gamma) \equiv \frac{1}{\pi\gamma}\left[(1 - \gamma \cot \gamma)^2 + \gamma^2\right] \qquad \text{for } 0 \leq \gamma < \pi \tag{59}$$

Upon defining $V_s^+(\eta)$ by

$$V_s^+(\eta) \equiv V_\infty \left|\zeta^+(z^S)\right| \qquad \text{for } 0 \leq \eta < \pi \tag{60}$$

and using equations (15), (16), (17), and (53), equation (49) becomes

$$\left[\frac{V_s^+(\eta)}{V_\infty}\right]^2 = \left|\zeta_0^S(\eta)\right|^2 \left\{1 + \epsilon + 2\epsilon \, \mathcal{R}e\left[\Theta^+(\eta) - \Lambda(\eta) I(\eta)\right]\right\} \qquad \text{for } 0 \leq \eta < \pi \tag{61}$$

where

$$\Lambda(\eta) \equiv \frac{\pi \Delta \sin^2 \eta}{(\sin \eta - \eta e^{-i\eta})(\eta e^{-i\eta} + \Delta \sin \eta)} \qquad \text{for } 0 \leq \eta < \pi \tag{62}$$

Let p_o be the pressure far inside the orifice (the point H in fig. 2). Since the velocity is zero there, it is clear that $p_o = P_j$. Hence, it follows from equation (2) that the pressure at the point (x_s, y_s) on the slip line $p(x_s, y_s)$ is given by

$$\frac{p_o - p(x_s, y_s)}{\frac{1}{2}\rho V_\infty^2} = \left|\zeta^+(z^S)\right|^2 = \frac{\left[V_s^+(\eta)\right]^2}{V_\infty^2} \tag{63}$$

Hence, let the pressure coefficient on the slip line C_{ps} be defined by

$$C_{ps} \equiv \frac{p_o - p(x_s, y_s)}{\frac{1}{2}\rho V_\infty^2} \tag{64}$$

Upon using equations (15), (17), (53), and (60), equation (50) becomes

$$\frac{\hat{S}(\eta)}{H_0 V_\infty} = \left(1 + \frac{\epsilon}{2}\right)\int_0^\eta \frac{1}{V_S^+(\gamma)}\, J(\gamma)d\gamma \qquad \text{for } 0 \le \eta < \pi \tag{65}$$

For convenience, the most important equations of this section are now summarized.

SUMMARY OF EQUATIONS

$$\left.\begin{aligned} a &= \frac{1}{\pi}\left[(1 - \Delta)\ln \Delta + 2(1 + \Delta)\right] \\ b &= \Delta - 1 \end{aligned}\right\} \qquad \text{for } 0 < \Delta \tag{20}$$

$$\zeta_0(T) = \frac{T}{T - \Delta} \qquad \text{for } \mathcal{Im}\, T \ge 0 \tag{16}$$

$$z(T) = \frac{1}{\pi}\left[T + (1 - \Delta)\ln T + \frac{\Delta}{T} + (1 + \Delta)\right] + i(\Delta - 1) \tag{19}$$

$$h = 1 - \frac{\epsilon}{\pi}\,\mathcal{Im}\int_0^\pi \Gamma(\eta)\left(\frac{1}{\eta} - \cot\eta - i\right)d\eta \tag{66}$$

$$\Gamma(\eta) = -i\Delta(\eta + \Delta \sin\eta\, e^{i\eta})\frac{\sin^2\eta}{\eta^2} \qquad \text{for } 0 \le \eta < \pi \tag{52}$$

$$\Theta^+(\eta) = \frac{1}{2}\Gamma(\eta) + \frac{P.V.}{2\pi i}\int_0^\pi \frac{\Gamma(\gamma)M(\gamma)d\gamma}{\gamma\cot\gamma - \eta\cot\eta - i(\gamma - \eta)}$$

$$- \frac{1}{2\pi i}\int_0^\pi \frac{\overline{\Gamma(\gamma)M(\gamma)}d\gamma}{\gamma\cot\gamma - \eta\cot\eta + i(\gamma + \eta)} \qquad \text{for } 0 \le \eta < \pi \tag{54}$$

where

$$M(\eta) \equiv \frac{1}{\sin^2\eta}(\gamma - \cos\eta \sin\eta) + i \tag{67}$$

$$\left.\begin{aligned} z_0^S(\eta) &\equiv z\left(-\frac{\eta}{\sin\eta} e^{-i\eta}\right) \\ \zeta_0^S(\eta) &\equiv \zeta_0\left(-\frac{\eta}{\sin\eta} e^{-i\eta}\right) \end{aligned}\right\} \quad \text{for } 0 \leq \eta < \pi \tag{56}$$

$$V_s^+(\eta) = |\zeta^+(z^S)| V_\infty \tag{60}$$

$$J(\gamma) = \frac{1}{\pi\gamma}\left[(1 - \gamma \cot\gamma)^2 + \gamma^2\right] \tag{59}$$

$$\Lambda(\eta) = \frac{\pi\Delta \sin^2\eta}{(\sin\eta - \eta e^{-i\eta})(\eta e^{-i\eta} + \Delta \sin\eta)} \quad \text{for } 0 \leq \eta < \pi \tag{62}$$

$$I(\eta) = \int_0^\eta \Theta^+(\gamma) J(\gamma) d\gamma \tag{58}$$

$$z^S = z_0^S(\eta) - \epsilon \frac{I(\eta)}{\zeta_0^2(\eta)} \quad \text{for } 0 \leq \eta < \pi \tag{57}$$

$$\left[\frac{V_s^+(\eta)}{V_\infty}\right]^2 = C_{ps} = |\zeta_0^S(\eta)|^2 \left\{1 + \epsilon + 2\epsilon \, Re\left[\Theta^+(\eta) - \Lambda(\eta) I(\eta)\right]\right\} \quad \text{for } 0 \leq \eta < \pi \tag{61}$$

$$\frac{\hat{S}}{V_\infty H_0} = \left(1 + \frac{\epsilon}{2}\right) \int_0^\eta \frac{1}{V_s^+(\gamma)} J(\gamma) d\gamma \quad \text{for } 0 \leq \eta < \pi \tag{65}$$

where equations (55) and (43) have been substituted into equation (11) to obtain equation (66).

RESULTS AND DISCUSSION

The numerical calculations were performed by using complex arithmetic. Hence, there is no need to separate the real and imaginary parts of the various formulas given in the preceding section. Equations (20) are used to calculate the orifice offset ratio $B/A = b/a$ for various values of the parameter Δ. However, it is more convenient to present the results in terms of the orifice orientation angle defined as $\tan^{-1} B/A$. A plot of the orifice angle against the parameter Δ is presented in figure 8. The orifice angle completely fixes the geometry of the problem. Hence, once the geometry of the orifice is set, the parameter Δ can be determined from figure 8. This parameter is the one which appears naturally in the formulas which are used to calculate the various physical quantities of interest. The only other parameter appearing in the problem is ϵ which gives a measure of the difference between the total pressure in the jet and the total pressure in the mainstream. This parameter is defined by equation (1) as

$$\epsilon = \frac{P_j - P_\infty}{\frac{1}{2}\rho V_\infty^2}$$

Equation (52) is used to calculate $\Gamma(\eta)$ for various values of Δ and these values of $\Gamma(\eta)$ are used together with equation (67) to calculate $\Theta^+(\xi)$ and h for various values of

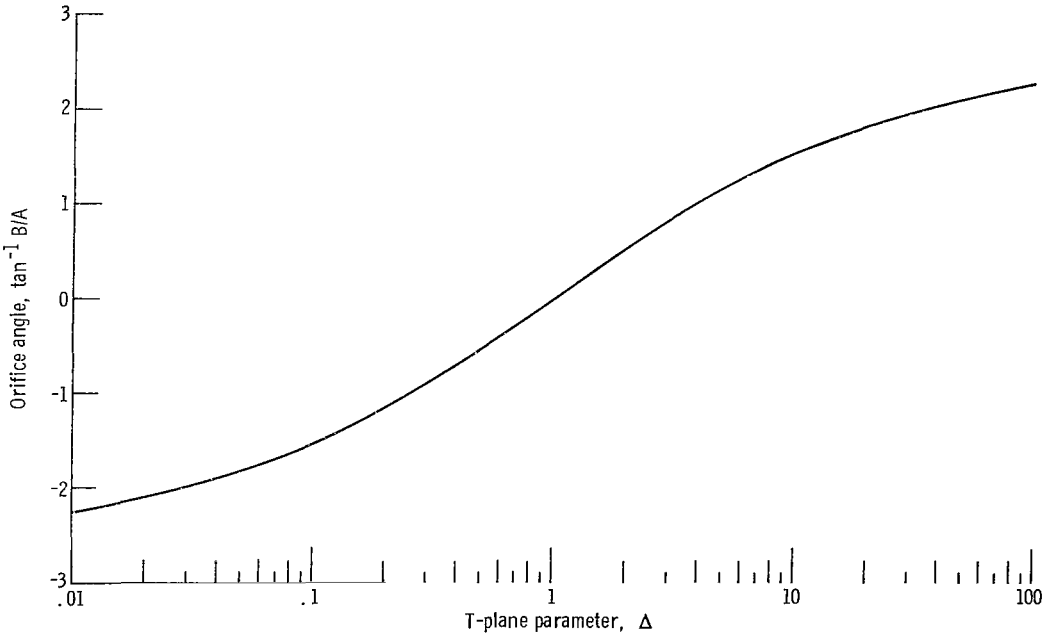

Figure 8. - Dependence of orifice angle on parameter Δ.

Δ from equations (54) and (66), respectively. All the physical quantities presented in the plots are determined by these latter two quantities.

Now for two-dimensional jets, the jet contraction ratio is defined as the asymptotic jet thickness divided by the length of the orifice. Hence, the jet contraction ratio is

$$\frac{H}{\sqrt{A^2 + B^2}} = \frac{h}{\sqrt{a^2 + b^2}}$$

Substituting equations (20) and (66) into this formula gives the jet contraction ratio as a function of Δ and ϵ or in view of figure 8 as a function of $\tan^{-1} B/A$ and ϵ. These results are presented in figure 9. It can be seen from figure 9 that, as in the case of the separated jet discussed in reference 1, for positive values of the orifice angle small changes of ϵ result in large changes in the contraction ratio, the effect becoming more marked as the orifice angle is increased. The opposite conclusion holds for negative values of the orifice angle. However, this effect is not nearly so marked as that of reference 1. Figure 9 also shows that, as in the case of the separated jet, for a given orifice angle increasing ϵ always results in an increase in the jet contraction ratio. This increase is negligible, however, for orifice angles less than -1.6 radians. Figure 9 shows that the jet contraction ratio is a maximum for an orifice angle of -1.2 radians and falls off markedly when the orifice angle is changed.

The parametric equations (with parameter η) for the slip line are obtained by substituting equations (19), (16), and (58) into equation (57) and using definitions (56) and the

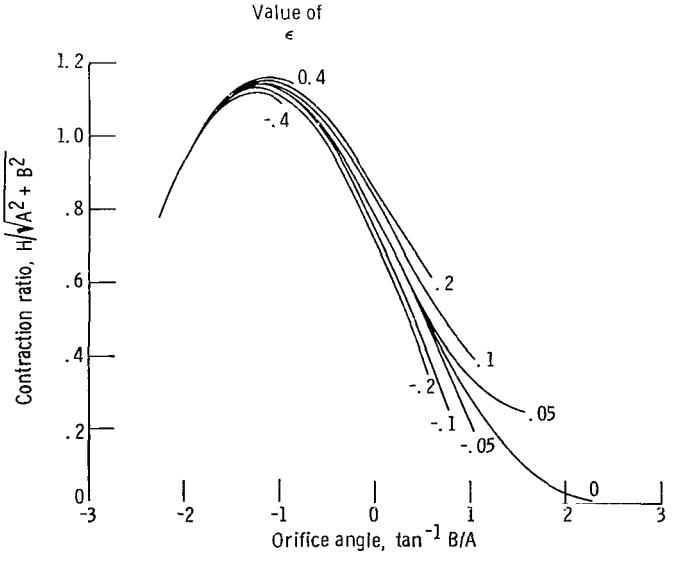

Figure 9. - Jet contraction ratio.

expression for $\Theta^{+}(\xi)$ discussed previously. The resulting expression determines the boundary of the jet. The shapes of the jet boundaries for various values of the parameters ϵ and B/A are shown in figures 10(a) to (i). Figure 10(a) corresponds to a jet injected normal to the mainstream B = 0. Figures 10(b) to (e) are for negative orifice angles (i.e., jet injected downstream) and figures 10(f) to (i) are for positive orifice angles (i.e., jet injected upstream). The configurations shown in figures 10(g) to (i) may be strongly modified by viscous effects. Figures 10(a) and (f) show that, as in the case of the separated jet discussed in reference 1, when the orifice angle is greater than or equal to zero a small change in the total pressure within the jet results in a fairly large change in both the jet penetration and jet thickness. This effect becomes more pronounced as the orifice angle is increased. However, the effect is not as marked as in the case of a separated jet. The figures also show that turning the jet into the main stream tends to markedly decrease the flow in the jet. The extreme sensitivity of the flow configuration to ϵ at large positive orifice angles indicates that the perturbation analysis will break down when the orifice angle is large enough.

The pressure coefficient on the slip line is obtained as a function of the distance along the slip line in parametric form from equations (61) and (65) after using definitions (52), (54), (56), and (58). The results of these calculations are shown in figures 11(a) to (h). Each figure is drawn for a different orifice angle. These curves contain all the information necessary for calculating the viscous boundary layer along the slip line. The curves show that for a fixed orifice angle the velocity at both the upstream edge of the orifice and at the downstream end of the slip line increases with increasing ϵ. For negative orifice angles the velocity tends to be relatively constant along the slip line, exhibiting a slight dip at the upstream edge of the orifice. As the orifice angle is increased toward zero the variation of velocity along the slip line becomes more pronounced. For nonnegative values of the orifice angle there is a definite peak in the velocity profiles which becomes more marked as the orifice angle is increased. This peak is attributed to the fact that the velocity is infinite at the downstream edge of the orifice. Since this point moves closer to the slip line as the orifice angle is increased, the velocity along the slip line becomes more peaked as the orifice angle increases. The contrast between the velocities (pressure coefficients) on the slip lines of the attached and separated jets is illustrated in figure 12 for zero orifice angle. The pressure coefficient of the separated jet rises monotonically to 1 far downstream. This smoother behavior can be attributed to the presence of the wake which adjusts in shape to keep the velocity of the turning jet from getting too large and the pressure from dropping too far below the static pressure of the stream. If the downstream wall is actually very thin, viscous effects will very likely cause the formation of a separation bubble at the lip. In that event, the velocity distribution on the slip line will fall between the two extremes shown in the figure.

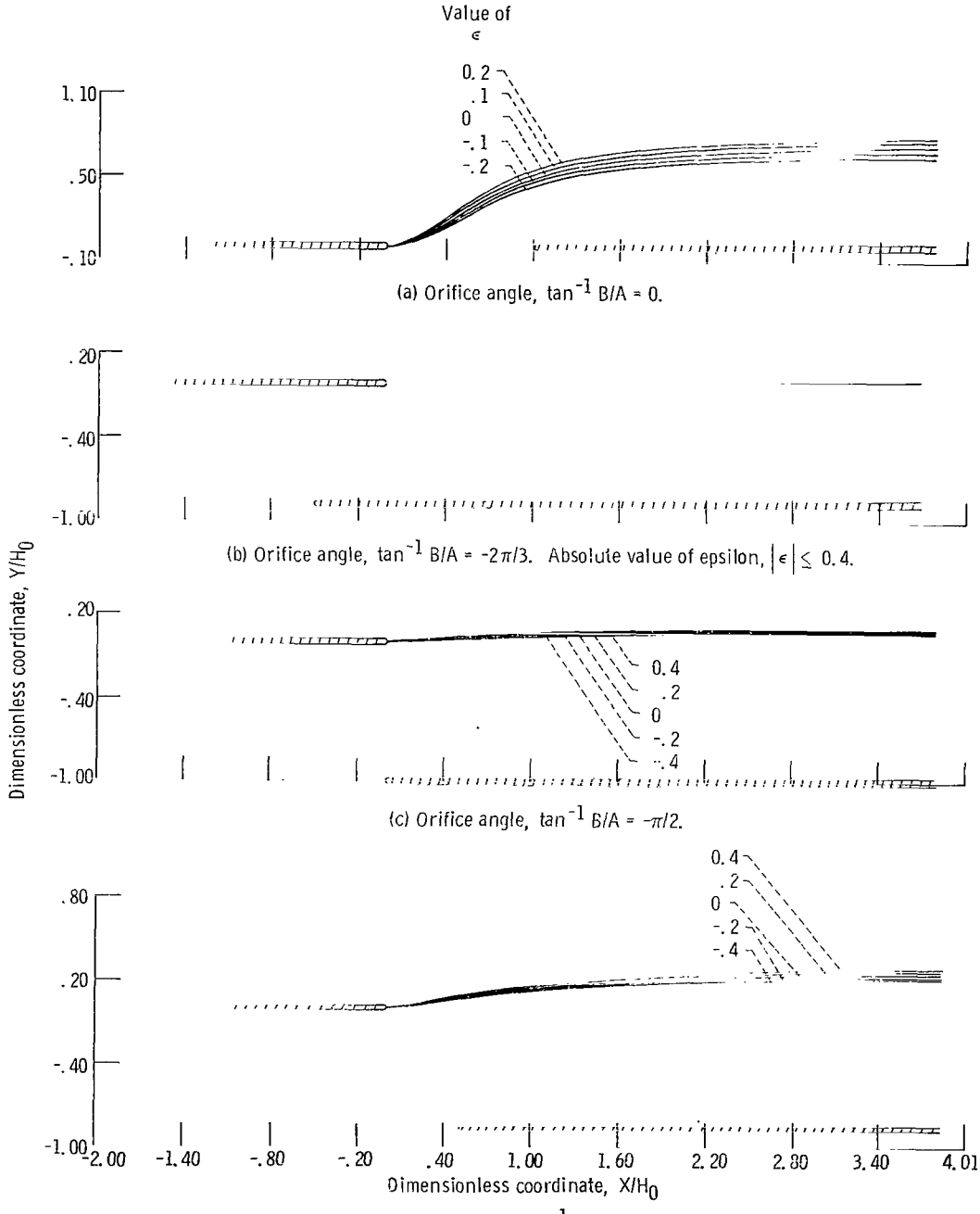

Figure 10. - Jet contours for varying orifice angles and varying values of ϵ.

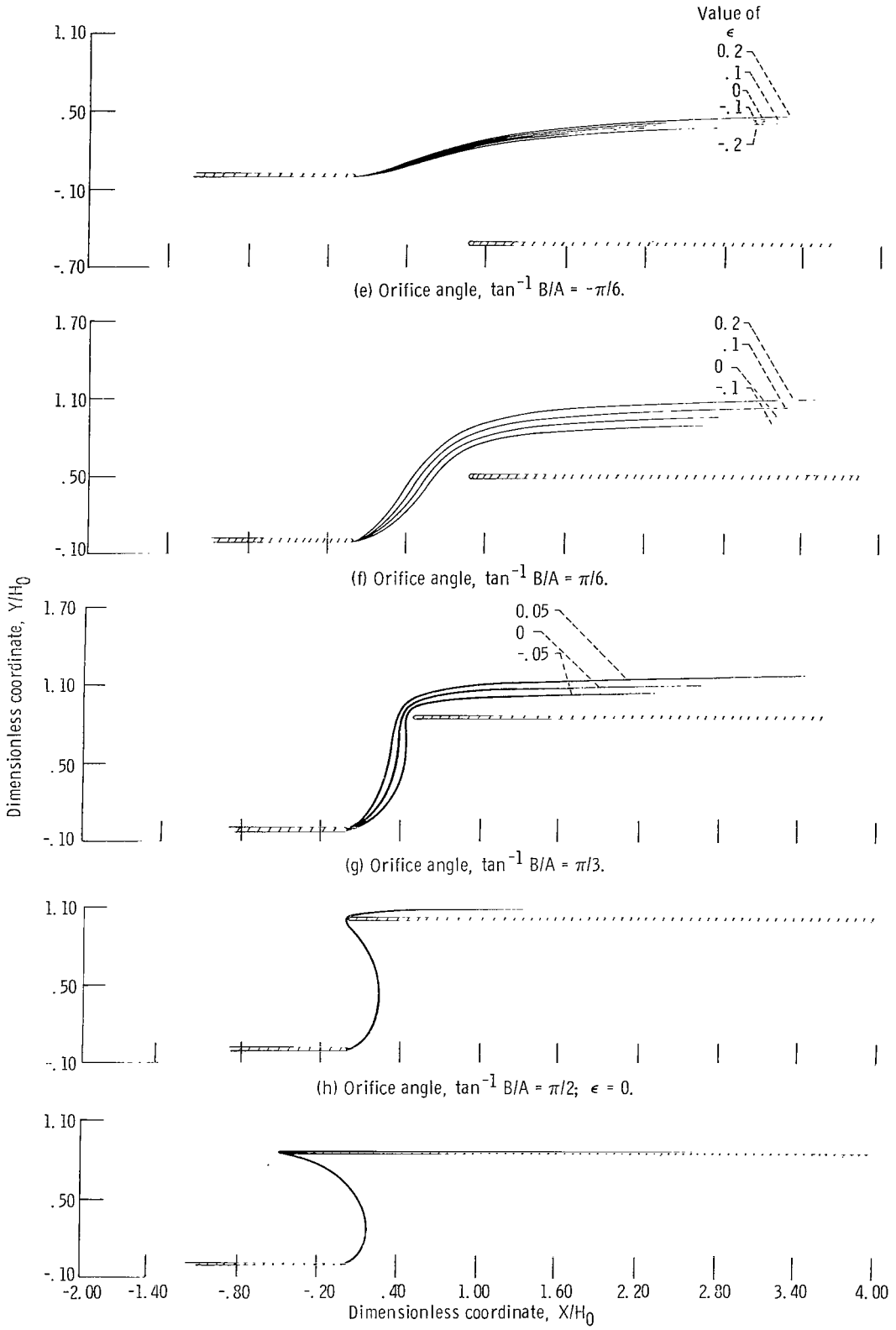

Figure 10. - Concluded.

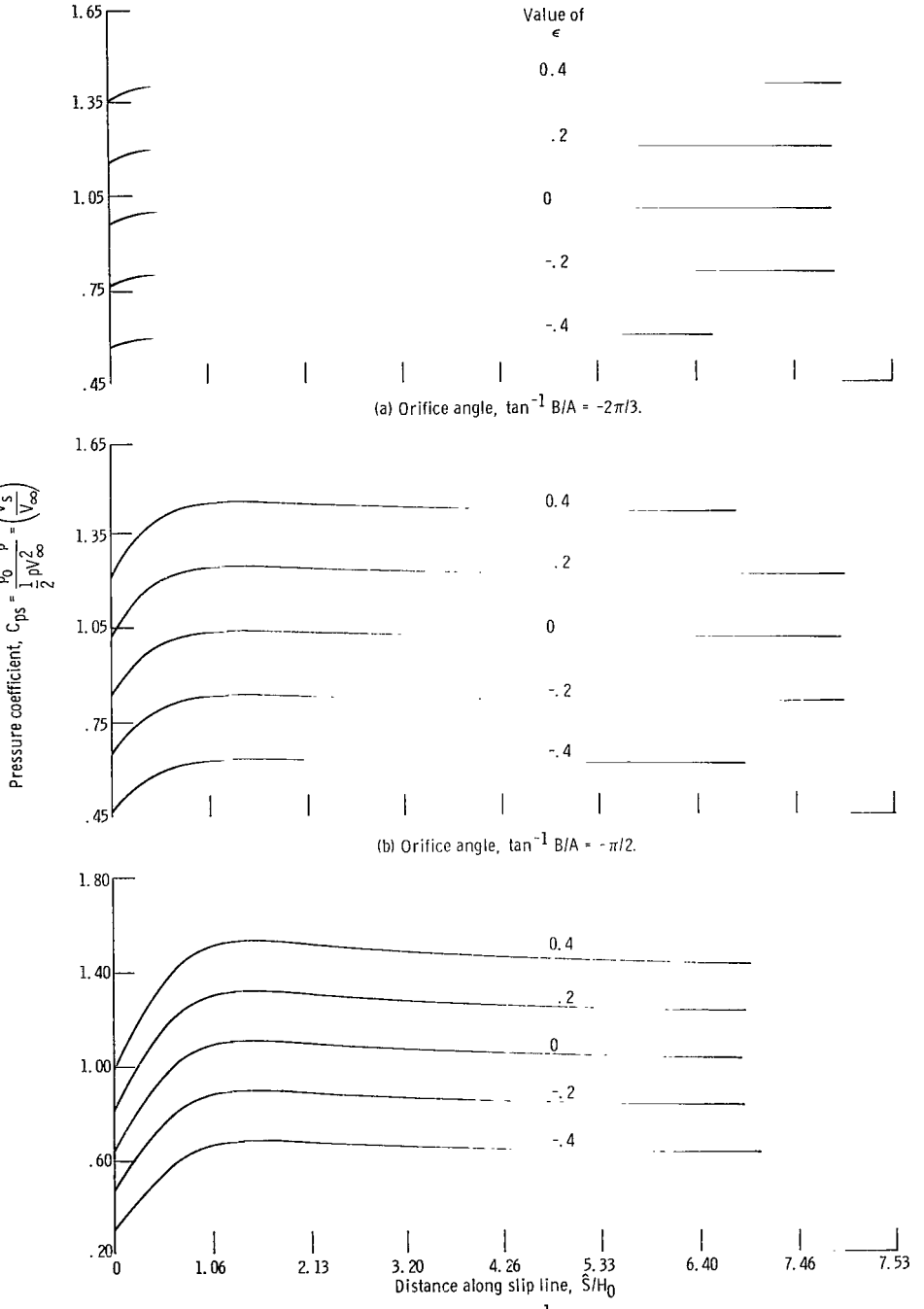

Figure 11. - Pressure coefficients on slip lines of jets for varying orifice angles and varying values of ϵ.

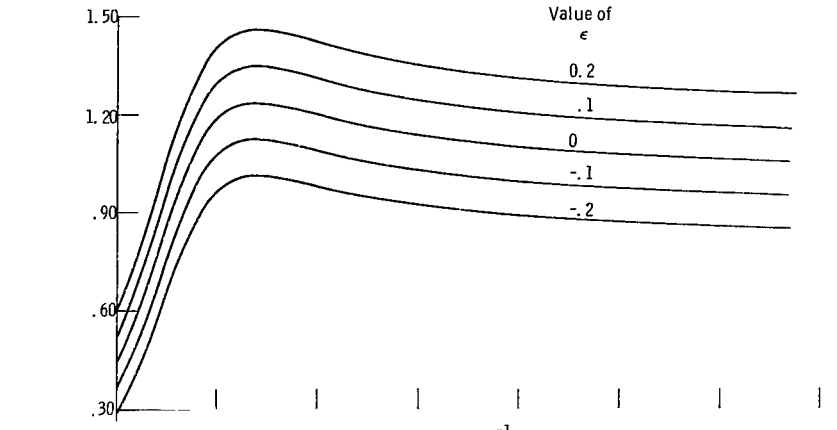

(d) Orifice angle, $\tan^{-1} B/A = -\pi/6$.

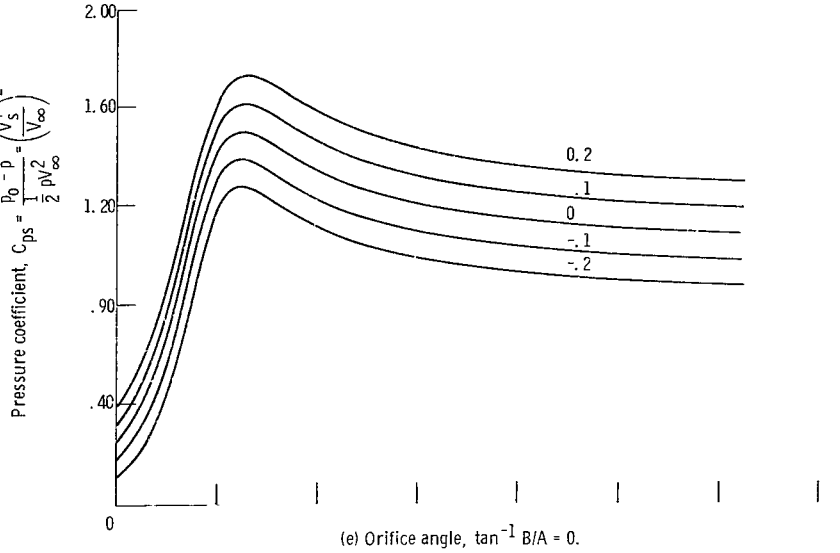

(e) Orifice angle, $\tan^{-1} B/A = 0$.

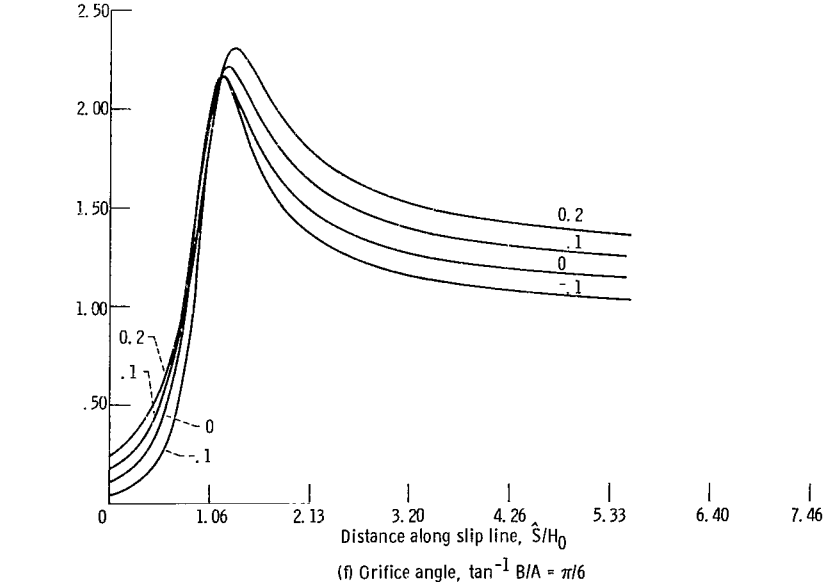

(f) Orifice angle, $\tan^{-1} B/A = \pi/6$

Figure 11. - Continued.

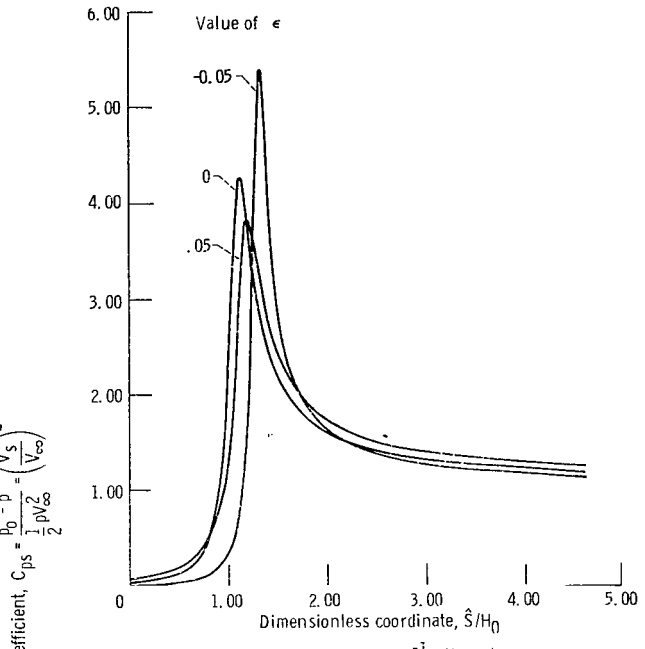

(g) Orifice angle, $\tan^{-1} B/A = \pi/3$.

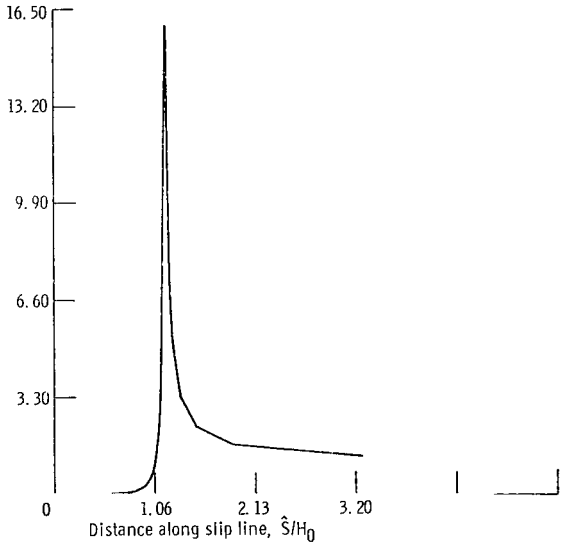

(h) Orifice angle, $\tan^{-1} B/A = \pi/2$; $\epsilon = 0$.

Figure 11. - Concluded.

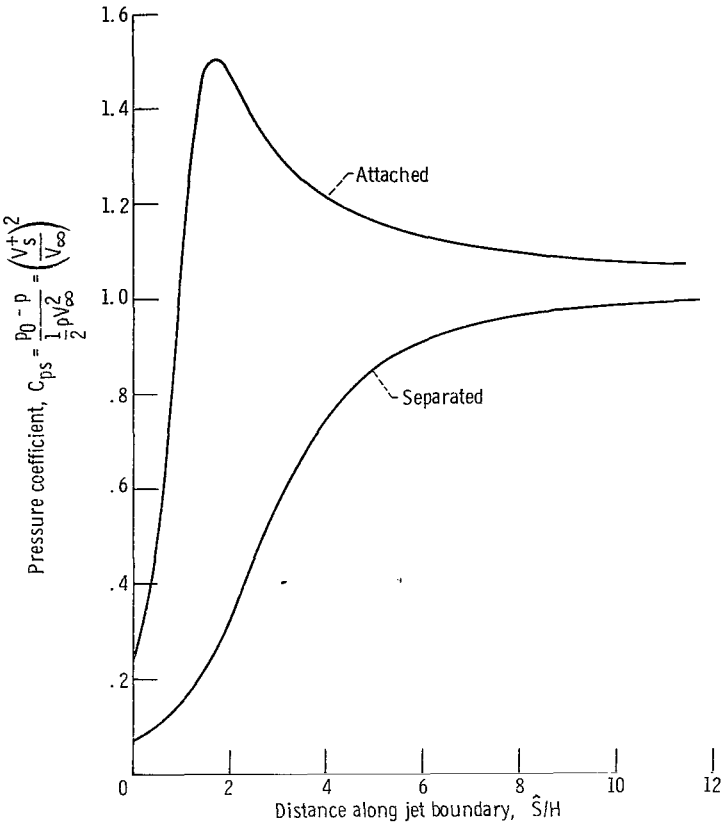

Figure 12. - Pressure coefficients of attached and separated jets. Orifice angle, $\tan^{-1} B/A = 0$; $\epsilon = 0$.

CONCLUDING REMARKS

A procedure developed in reference 1 has been applied to obtain a solution to the problem of a two-dimensional inviscid jet injected from an orifice at an oblique angle to a moving stream for the case where the jet does not separate from the downstream edge of the orifice. The analysis shows a peaking of the pressure coefficient along the slip line which increases as the orifice is tilted into the stream. Tilting the jet into the stream also makes the jet contraction ratio more sensitive to changes in total pressure in the jet.

Lewis Research Center,
National Aeronautics and Space Administration,
Cleveland, Ohio, August 12, 1969,
129-01.

REFERENCES

1. Goldstein, M. E.; and Braun, W.: Injection of an Inviscid Separated Jet at an Oblique Angle to a Moving Stream. NASA TN D-5460, 1969.

2. Batchelor, G. K.: An Introduction to Fluid Dynamics. Cambridge University Press, 1967, pp. 410-412.

3. Birkhoff, Garrett; and Zarantonello, E. H.: Jets, Wakes, and Cavities. Academic Press, 1957.

4. Ehrich, Fredric F.: Penetration and Deflection of Jets Oblique to a General Stream. J. Aeron. Sci., vol. 20, no. 2, Feb. 1953, pp. 99-104.

5. Churchill, Ruel V.: Complex Variables and Applications. Second ed., McGraw-Hill Book Co., Inc., 1960.

6. Muskhelishvili, Nikolai I.: Singular Integral Equations. P. Noordhoff, Ltd., 1953.

NASA-Langley, 1969 —— 12 E-5106

"The aeronautical and space activities of the United States shall be conducted so as to contribute . . . to the expansion of human knowledge of phenomena in the atmosphere and space. The Administration shall provide for the widest practicable and appropriate dissemination of information concerning its activities and the results thereof."

—NATIONAL AERONAUTICS AND SPACE ACT OF 1958

NASA SCIENTIFIC AND TECHNICAL PUBLICATIONS

TECHNICAL REPORTS: Scientific and technical information considered important, complete, and a lasting contribution to existing knowledge.

TECHNICAL NOTES: Information less broad in scope but nevertheless of importance as a contribution to existing knowledge.

TECHNICAL MEMORANDUMS: Information receiving limited distribution because of preliminary data, security classification, or other reasons.

CONTRACTOR REPORTS: Scientific and technical information generated under a NASA contract or grant and considered an important contribution to existing knowledge.

TECHNICAL TRANSLATIONS: Information published in a foreign language considered to merit NASA distribution in English.

SPECIAL PUBLICATIONS: Information derived from or of value to NASA activities. Publications include conference proceedings, monographs, data compilations, handbooks, sourcebooks, and special bibliographies.

TECHNOLOGY UTILIZATION PUBLICATIONS: Information on technology used by NASA that may be of particular interest in commercial and other non-aerospace applications. Publications include Tech Briefs, Technology Utilization Reports and Notes, and Technology Surveys.

Details on the availability of these publications may be obtained from:

SCIENTIFIC AND TECHNICAL INFORMATION DIVISION

NATIONAL AERONAUTICS AND SPACE ADMINISTRATION

Washington, D.C. 20546